

Proceeding Paper

# Modeling and Numerical Simulation of a $\text{CH}_3\text{NH}_3\text{SnI}_3$ Perovskite Solar Cell Using the SCAPS1-D Simulator <sup>†</sup>

Selma Rabhi <sup>1,2,\*</sup>, Hichem Benzouid <sup>3</sup>, Abdelhadi Slami <sup>4</sup> and Karima Dadda <sup>1</sup>

<sup>1</sup> LMSCMO, University of Science and Technologie Haouri BOUMEDIEN, Algiers, Algeria; email1@email.com (K.D.)

<sup>2</sup> Dr. YAHIA Fares University, Medea, Algeria

<sup>3</sup> Laboratory of Metallurgy and Materials Engineering, University of Badji Mokhtar (UBMA), Annaba, Algeria; email2@email.com (H.B.)

<sup>4</sup> Material and Renewables Energies "URMER, University of Tlemcen, Algeria; email3@email.com (A.S.)

\* Correspondence: selma.rabhi@ensmm-annaba.dz or rabhi.selma@univ-medea.dz

<sup>†</sup> Presented at the 4th International Electronic Conference on Applied Sciences, 27 October–10 November 2023; Available online: <https://asec2023.sciforum.net/>.

**Abstract:** In this work, our aim is to design and numerical simulation of a solar cell using the SCAPS-1D simulation program. The studied solar cell has an N-I-P type structure, with its active layer based on a hybrid (organic-inorganic) semiconductor called "methylammonium tin triiodide perovskite"  $\text{CH}_3\text{NH}_3\text{SnI}_3$  has known  $\text{MASnI}_3$ . This semiconductor is known by its efficiency in the field of photovoltaic thanks to its good proprieties such as high absorption, direct bang-gap and facilities of elaboration. The objective of this study is primarily focused on improving the performance of the solar cell, specifically enhancing the photovoltaic parameters of perovskite solar cells. The objective of this study is primarily focused on improving the performance of the solar cell, specifically enhancing the reproducibility and stability of perovskite solar cells, as they tend to degrade rapidly. To achieve this, we have proposed the use of ZnO and Spiro-OMeTAD as charge transport layers (ETL and HTL, respectively) and varying the thickness of the active layer to obtain the optimal parameters that ensure the proper functioning of the cell.

**Keywords:** SCAPS-1D; hybrid; perovskite; photovoltaics; ETL; HTL

**Citation:** Rabhi, S.; Benzouid, H.; Slami, A.; Dadda, K. Modeling and Numerical Simulation of a  $\text{CH}_3\text{NH}_3\text{SnI}_3$  Perovskite Solar Cell Using the SCAPS1-D Simulator. *Eng. Proc.* **2023**, *52*, x. <https://doi.org/10.3390/xxxxx>

Academic Editor(s): Name

Published: date



**Copyright:** © 2023 by the authors. Submitted for possible open access publication under the terms and conditions of the Creative Commons Attribution (CC BY) license (<https://creativecommons.org/licenses/by/4.0/>).

## 1. Introduction

The revolution in the solar cell industry is to make solar cells more efficient and punchier and at low cost. Perovskite-based solar cells could revolutionize this industry thanks to their interesting physico-chemical properties. The perovskite is the active layer in the solar cell, therefore, the coupling between the development and the study of the different properties of this layer in order to find the optimal conditions for the development of the perovskite layer contributes to the manufacture of an efficient solar cell [1]. Perovskite has a structure designated by the formula of  $\text{AMX}_3$ , where A is the cation (Cs, Rh, MA:  $\text{CH}_3\text{NH}_3$  or else the FA: for  $\text{CH}(\text{NH}_2)_2$ , and M is a cationic metal ( $\text{Pb}^{2+}$ ,  $\text{Sn}^{2+}$ ,  $\text{Ge}^{2+}$ ) and X is an oxide or a halide (I, Br, Cl...). Its structure is an ionic structure, where the  $\text{MX}_6$  form an octahedron with M located in the center of the octahedron and X are linked to the vertices of the cube around M. It is a tetragonal structure which contains an octahedral structure [2,3]. For these solar cells, the most commonly used component as the active layer is  $\text{CH}_3\text{NH}_3\text{PbI}_3$ , referred to as  $\text{MAPbI}_3$ , or Methyl Ammonium Lead Iodide. However, perovskites based on  $\text{MAPbI}_3$  are toxic due to the presence of Pb, which can destabilize the continued commercialization of these cells. One of the alternative solutions is a perovskite material containing tin (Sn) instead of lead (Pb), known as Methyl Ammonium Tin Iodide ( $\text{CH}_3\text{NH}_3\text{SnI}_3$  or  $\text{MASnI}_3$ ). Many researchers have started to develop cells based

on  $\text{CH}_3\text{NH}_3\text{SnI}_3$ , and this is what we have also attempted to do [4]. Tin occurs naturally and has almost the same electronic properties as lead (Pb). Moreover, Sn-based perovskite solar cells (PSCs) exhibit good absorption in the visible light spectrum and high charge mobilities, resulting in high solar cell efficiency [5–7]. The transport layers and the architecture also play a significant role in the efficiency of solar cells. In this work, we will present and discuss the results of our simulation for  $\text{CH}_3\text{NH}_3\text{SnI}_3$ -based PSCs.

## 2. Device Simulation Parameters

Numerical modeling has shown to be beneficial for the investigation of the physical properties and construction of various solar cells made from different materials. Meanwhile, Solar Cell Capacitance Simulator SCAPS-1D (ELIS, University of Ghent, Belgium [8]) has demonstrated its efficacy in modeling a range of research systems, and it has become a widely used as simulation tool for solar cell researchers due to its specialized functionality for semiconductor devices. A structure of the  $\text{CH}_3\text{NH}_3\text{SnI}_3$ -based PSC employed in this study is shown in **Error! Reference source not found.a**, where the photovoltaic cell configuration is as follows the  $\text{ZnO}/\text{CH}_3\text{NH}_3\text{SnI}_3/\text{Spiro-OMeTAD}/\text{Au}$ , the layers are stacked in the N-I-P structure. These materials exhibit favorable electronic properties, which the ETL, ZnO possesses optical and electronic properties appreciated in the field of electronics. For the HTL, the most commonly used material in perovskite photovoltaic is Spiro-OMeTAD, as it is straightforward to implement and efficient in cells. However, the full device structure was simulated in SCAPS 1D by solving Poisson, electron and hole continuity equations with inputs based on literature values (**Error! Reference source not found.**). While, the SCAPS-1D software uses all the inputs to explore fundamental properties such as the short-circuit current  $J_{\text{sc}}$ , the open-circuit voltage  $V_{\text{oc}}$ , the power conversion efficiency of the device PCE, the quantum efficiency QE and the fill factor FF.

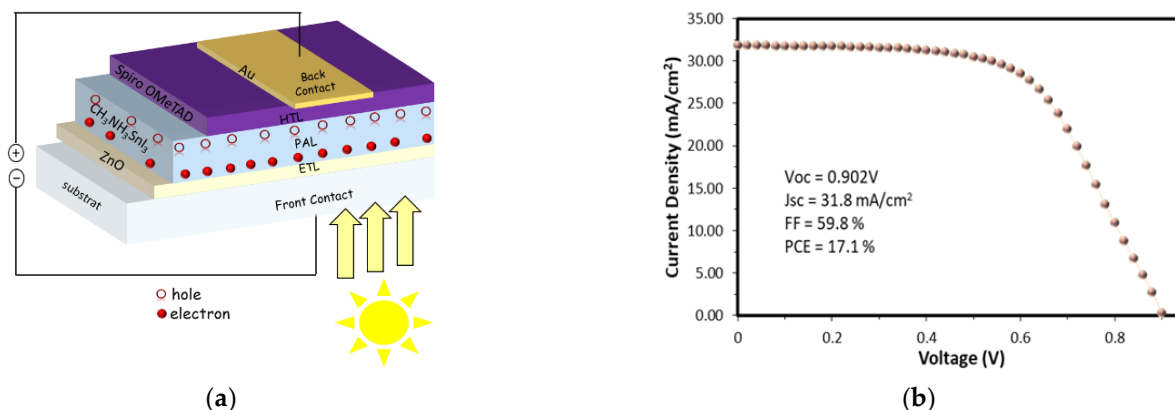


**Figure 1.** (a) Schematic of main device and (b) Presents J-V characteristic of  $\text{MAPbI}_3$ -based solar cell with the photovoltaic parameters.

**Error! Reference source not found.** shows the inputs parameters of the layers that make up the perovskite solar cell; we will use these inputs to extract the performance parameter of PSCs such as the  $J_{\text{sc}}$ ,  $V_{\text{oc}}$ , FF and PCE.

**Table 1.** Inputs parameters of all layers in PSCs [9–12].

Parameters	ZnO	$\text{CH}_3\text{NH}_3\text{SnI}_3$	Spiro-OMeTAD
Thickness (nm)	500	450	0.350
Bandgap (eV)	3.47	1.3	3.2
Electron affinity (eV)	4.3	4.2	2.1
Dielectric permittivity (relative)	9	10	3
CB effective density of states ( $1/\text{cm}^3$ )	$2E+18$	$1.0E+19$	$2.5E+18$

<b>VB effective density of states (1/cm<sup>3</sup>)</b>	1.8E+20	1.0E+18	1.8E+19
<b>Electron thermal velocity (cm/s)</b>	1E+7	1E+7	1E+7
<b>Hole thermal velocity (cm/s)</b>	1E+7	1E+7	1E+7
<b>Electron mobility (cm<sup>2</sup>/Vs)</b>	1.0E+2	1.6E+0	2.0E-4
<b>Hole mobility (cm<sup>2</sup>/Vs)</b>	2.5E+1	1.6E+0	2.0E-4
<b>Shallow uniform acceptor density, N<sub>A</sub> (1/cm<sup>3</sup>)</b>	0	3.0E+15	1.0E+20
<b>Shallow uniform donor density N<sub>D</sub> (1/cm<sup>3</sup>)</b>	1E+19	3.0E+15	0
<b>Defect type</b>	—	Neutral	Neutral
<b>Capture cross section electrons (cm<sup>2</sup>)</b>	—	1E-16	1E-15
<b>Capture cross section holes (cm<sup>2</sup>)</b>	—	1E-16	1E-15
<b>Energy level with respect to reference (eV)</b>	—	0.7	0.10
<b>N<sub>i</sub> total (1/cm<sup>3</sup>) uniform</b>	—	4.5E+16	1.00E+14

### 3. Results and Discussion

After selecting the inputs parameters of N-, I- and P-layer that we need for SCAPS, we constructed the structure of the Sn-based PSC as presented on Figure 1a. The cell is illuminated from one side only (front side on the HTL side), and we calculated the current-voltage density characteristic (J-V) for the very first time. **Error! Reference source not found.** shows the current-voltage (J-V) characteristic of this cell under illumination by the AM 1.5 solar spectrum and a power density of 1000 w/m<sup>2</sup> [13]. From the J-V characteristics provided by SCAPS-1D in Figure 2, we were able to determine photovoltaic performance such as J<sub>sc</sub>, V<sub>oc</sub>, FF, and PCE. Where, the PCE of this cell is ≈17%, which means that the solar cell can convert only 17% of the light into usable electricity. This efficiency is low compared with the theoretical works on PSCs employing other materials as ETL and the expectation for the CH<sub>3</sub>NH<sub>3</sub>SnI<sub>3</sub>-based PSC. In recent times, Omarova et al. show that the PSCs with TiO<sub>2</sub>/CH<sub>3</sub>NH<sub>3</sub>SnI<sub>3</sub>/Cu<sub>2</sub>O device structure offer an excellent PCE of ~27% [14]. Their results explain that the TiO<sub>2</sub>-containing device efficiently decreases the charge recombination, which means an enhancement in the PV performance. In addition, Hui-Jing Du et al. using TiO<sub>2</sub> as ETL with CH<sub>3</sub>NH<sub>3</sub>SnI<sub>3</sub> PSCs offered PCE of 23.36% after the optimization of PSC [15]. Otherwise, A V<sub>oc</sub> of ≈0.9 V, represents the maximum voltage measured across the solar cell when no load is connected. An open circuit voltage is almost of the order and indicates that the solar cell is not capable of generating a significant voltage. Whereas, A J<sub>sc</sub> of almost 32 mA/cm<sup>2</sup> for a CH<sub>3</sub>NH<sub>3</sub>SnI<sub>3</sub>-based PSC is generally considered to be quite good. However, FF of ≈60%: The fill factor is a measure of the solar cell's efficiency in terms of energy management. A FF of 60% is considered relatively low because it only exceeds the average by a small percent and this shows that the solar cell is not using the available energy efficiently.

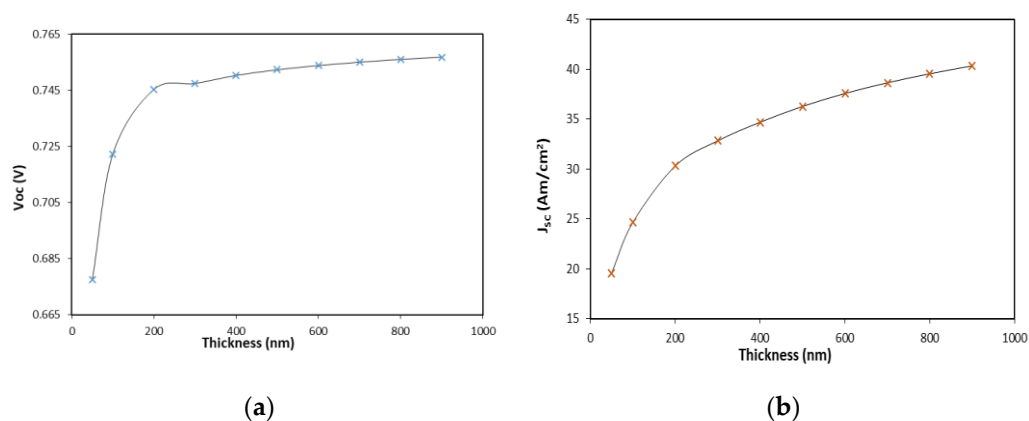


**Figure 2.** (a) Presents the variation of open circuit voltage as a function of thickness and (b) presents variation in current density as a function of thickness.

### 3.1. Performance of Optimized Parameters

Therefore, we will try to improve the performance of  $\text{CH}_3\text{NH}_3\text{SnI}_3$ -based PSC by optimizing some technological parameters of the absorber layer  $\text{CH}_3\text{NH}_3\text{SnI}_3$  as it is the main layer in the whole cell. Therefore, we will optimize the thickness of the  $\text{CH}_3\text{NH}_3\text{SnI}_3$  active layer to have its best characteristics to the aim to enhance the performance of the  $\text{CH}_3\text{NH}_3\text{SnI}_3$ -based PSC. We will also simulate the effect of temperature on the complete solar cell. We varied the thickness of the  $\text{CH}_3\text{NH}_3\text{SnI}_3$  active layer from 100 nm up to 900 nm in 100 nm increments.

To better visualize the effect of thickness on the performance of this photovoltaic cell, we have plotted the four performances as a function of thickness. Figures 2–4 show these performances ( $V_{\text{OC}}$ ,  $J_{\text{SC}}$ , FF and PCE). Figure 2a shows the open circuit voltage as a function of the thickness of the  $\text{CH}_3\text{NH}_3\text{SnI}_3$  active layer. We observe that this voltage increases as a function of thickness. This gradual increase in  $V_{\text{OC}}$  with increasing layer thickness goes from 0.6774 V to 0.7568 V. This means that there is a positive correlation between the thickness of the active layer and the open circuit voltage. This correlation may be due to the charge transport properties or to better light capture by the active layer. This result is logical because of the good general electronic properties of  $\text{CH}_3\text{NH}_3\text{SnI}_3$  active layer. With regard to the second performance, Figure 2b also shows the evolution of the  $J_{\text{SC}}$  as a function of the thickness of the active layer. A steady increase in short-circuit current is observed with increasing layer thickness, rising from 19.55  $\text{mA}/\text{cm}^2$  to 40.35  $\text{mA}/\text{cm}^2$  over the range 50 nm to 900 nm. This could be explained by the fact that the cell with a thicker active layer contains a greater quantity of material capable of generating current in response to illumination.

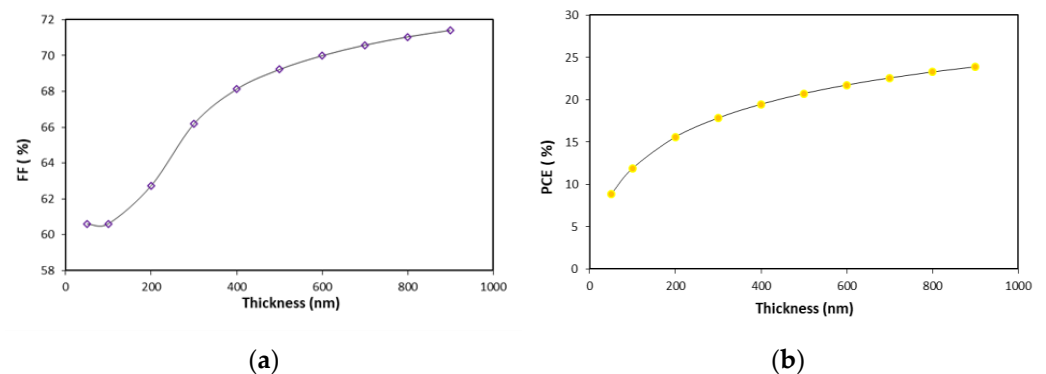


**Figure 3.** Presents the variation: (a) of Fill Factor as a function of thickness and (b) in Power Conversion Efficiency as a function of thickness.

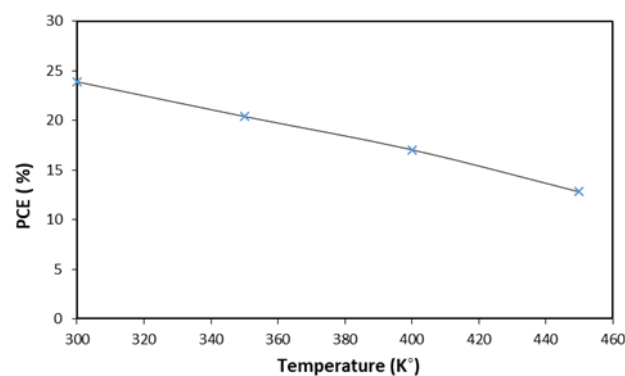


**Figure 4.** The influence of temperature increase on solar cell efficiency.

While, the fill factor FF (%) is shown in Figure 3a, with an increase from 60.59% to 71.41%. This means that the cell with an active layer thickness of 900 nm converts light

into energy at a rate of 71.41%. Now we come to the efficiency of the solar cell. As mentioned earlier, the PCE is a measure of the overall efficiency of a solar cell in converting light energy into electrical energy. The results presented in Figure 3b show a significant increase in efficiency with increasing film thickness, from 8.87% to 23.9%. This suggests that higher layer thicknesses can lead to better overall solar cell efficiency. Therefore, increasing the thickness of the  $\text{CH}_3\text{NH}_3\text{SnI}_3$  active layer, which is the absorbing layer in the solar cell, results in better absorption of sunlight. This results in greater photon capture, which increases the number of electron-hole pairs generated. As a result, the amount of solar energy converted into electricity increases, which translates into an increase in the electrical current produced [16]. One of the positive results of increasing the thickness of the active layer is an increase in the diffusion time of charge carriers in the cell. This means that charge carriers have a greater chance of interacting with current collection sites, reducing recombination losses [17,18]. It is important to note that increasing thickness also has limits. Beyond a certain thickness, the effect of increasing thickness on efficiency can decrease, or even become negative, due to reduced charge carrier collection or other undesirable effects. Optimal photovoltaic cell design must consider these factors to maximize overall efficiency. The choice of ETL and HTL layers and even contact materials play a very important role on solar cell parameters, in this thesis we have focused only on the effect of thickness on solar cell parameters [19]. As a result, these results indicate a correlation between the thickness of the  $\text{CH}_3\text{NH}_3\text{SnI}_3$  active layer and the performance of the overall perovskite solar cell. A greater thickness favors higher values of open circuit voltage, short circuit current density and overall efficiency. The good result is obtained for a  $\text{CH}_3\text{NH}_3\text{SnI}_3$  active layer thickness of 900 nm, so this thickness is the optimum value where at this thickness the  $\text{CH}_3\text{NH}_3\text{SnI}_3$ -based PSC has good photovoltaic performance.

### 3.2. The Effect of Temperature on Solar Cell Efficiency

In this section, we will analyse the effect of temperature on the efficiency of a perovskite solar cell with a  $\text{CH}_3\text{NH}_3\text{SnI}_3$  active layer thickness of 900 nm, whereas we varied the temperature from 300 K to 450 K with 50 K as steps. These results clearly indicate that increasing temperature has a negative impact on the performance of the  $\text{CH}_3\text{NH}_3\text{SnI}_3$ -based PSC. Higher temperature leads to a decrease in  $V_{oc}$ , FF and overall PCE. As well as the short circuit current density although it appeared relatively stable, but can also show a slight decrease at higher temperatures. Figure 4 shows significantly the decrease in PCE with increasing of temperature. However, these results are consistent with the negative effects of temperature on the performance of perovskite-based solar cells; increasing temperature can have a significant negative impact on overall cell efficiency. One of the main reasons for this is that  $\text{CH}_3\text{NH}_3\text{SnI}_3$  layer is temperature-sensitive materials [18,20,21], which means that their optoelectronic properties are affected by temperature variations.

## 4. Conclusions

In this work, we modeled and optimized a  $\text{CH}_3\text{NH}_3\text{SnI}_3$ -based perovskite solar cell using ZnO and Spiro-OMeTAD as the electron and hole transport layers, respectively using SCAPS software and we identified an optimal thickness of 900 nm which provided the  $\text{CH}_3\text{NH}_3\text{SnI}_3$  layer as an excellent light absorption. The modeled cell achieves high power conversion efficiency exceeding 24%, open-circuit voltage of 0.76 V, short-circuit current density of 40.35 mA/cm<sup>2</sup>, and fill factor of 71.41%. These high photovoltaic parameters demonstrate that  $\text{CH}_3\text{NH}_3\text{SnI}_3$ -based PSCs can match or even surpass their  $\text{CH}_3\text{NH}_3\text{PbI}_3$ -based counterparts and satisfy environmental concerns by being environmentally friendly. The proposed model of a tin-based PSC with an absorbing layer thickness of 900 nm, which is more standard in terms of fabrication and intending for further application in the development of environmentally-friendly and lead-free PSCs. With further optimization of thermal stability, interface engineering, and geometry, tin-based PSCs could become leading candidates for next-generation solar cells. The SCAPS simulations provide

critical insights to guide the experimental development of efficient, stable, and eco-friendly tin-based PSCs.

**Author Contributions:** S.R.: Supervision, Validation, Visualization, Writing—original draft. H.B.: Data acquisition, Formal analysis, Writing—review & editing. A.S.: Data acquisition, Formal analysis, Validation, Visualization. K.D.: Resources, Visualization, Writing—original draft. All authors have read and agreed to the published version of the manuscript.

**Funding:** This research received no external funding.

**Institutional Review Board Statement:** Not applicable.

**Informed Consent Statement:** Not applicable.

**Data Availability Statement:** Not applicable.

**Acknowledgments:** M Burgelman of the University of Gent in Belgium kindly provided the SCAPS-1D program. The authors express their gratitude to him.

**Conflicts of Interest:** The authors declare no conflict of interest.

## References

1. Selma, M.R. Etat de l' Art Des Couches Minces à Base Pérovskite Pour Des Applications Photovoltaïques Présenté Par. Master's Thesis, Université Frères Mentouri Constantine, Constantine, Algeria, 2015.
2. Kojima, A.; Teshima, K.; Shirai, Y.; Miyasaka, T. Organometal Halide Perovskites as Visible-Light Sensitizers for Photovoltaic Cells. *J. Am. Chem. Soc.* **2009**, *131*, 6050–6051. <https://doi.org/10.1021/ja809598r>.
3. Graetzel, M.; Malinkiewicz, O.; Yella, A.; Lee, Y.H.; Mi, G.; Nazeeruddin, M.K.; Bolink, H.J. Perovskite Solar Cells Employing Organic Charge-Transport Layers. *Nat. Photonics* **2014**, *8*, 128–132. <https://doi.org/10.1038/nphoton.2013.341>.
4. Zh, O.; Yerezhep, D.; Aldiyarov, A.; Golikov, O.; Tokmoldin, N. Performance Simulation of Eco-Friendly Solar Cells Based on  $\text{CH}_3\text{NH}_3\text{SnI}_3$ . *Eurasian Phys. Tech. J.* **2022**, *19*, 58–64. <https://doi.org/10.31489/2022No2/58-64>.
5. Deepthi Jayan, K.; Sebastian, V. Comprehensive Device Modelling and Performance Analysis of  $\text{MASnI}_3$  Based Perovskite Solar Cells with Diverse ETM, HTM and Back Metal Contacts. *Sol. Energy* **2021**, *217*, 40–48. <https://doi.org/10.1016/j.solener.2021.01.058>.
6. Rawat, S.; Shrivastav, N.; Madan, J. Analysis and Optimization of  $\text{MASnPbI}_3$ -Based Single Junction Solar Cells for High Power Conversion Efficiency. In Proceedings of the 2023 Second International Conference on Electrical, Electronics, Information and Communication Technologies (ICEEICT), Trichirappalli, India, 5–7 April 2023; pp. 1–3. <https://doi.org/10.1109/ICEEICT56924.2023.10157594>.
7. Shankar, G.; Kumar, P.; Pradhan, B. All-Perovskite Two-Terminal Tandem Solar Cell with 32.3% Efficiency by Numerical Simulation. *Mater. Today Sustain.* **2022**, *20*, 100241. <https://doi.org/10.1016/j.mtsust.2022.100241>.
8. Burgelman, M.; Nollet, P.; Degraeve, S. Modelling Polycrystalline Semiconductor Solar Cells. *Thin Solid Films* **2000**, *361*, 527–532. [https://doi.org/10.1016/S0040-6090\(99\)00825-1](https://doi.org/10.1016/S0040-6090(99)00825-1).
9. Anwar, F.; Mahbub, R.; Satter, S.S.; Ullah, S.M. Effect of Different HTM Layers and Electrical Parameters on ZnO Nanorod-Based Lead-Free Perovskite Solar Cell for High-Efficiency Performance. *Int. J. Photoenergy* **2017**, *2017*, 9846310. <https://doi.org/10.1155/2017/9846310> Research.
10. Takahashi, Y.; Obara, R.; Lin, Z.; Takahashi, Y. Charge-Transport in Tin-Iodide Perovskite  $\text{CH}_3\text{NH}_3\text{SnI}_3$ : Origin of High Conductivity Takahashi. *Dalt. Trans.* **2011**, *40*, 5563–5568. <https://doi.org/10.1039/c0dt01601b.1>.
11. Sabetvand, R.; Ghazi, M.E.; Izadifard, M. Studying Temperature Effects on Electronic and Optical Properties of Cubic  $\text{CH}_3\text{NH}_3\text{SnI}_3$  Perovskite. *J. Comput. Electron.* **2020**, *19*, 70–79. <https://doi.org/10.1007/s10825-020-01443-3>.
12. Slami, A. Comparative Study of Modeling of Perovskite Solar Cell with Different HTM Layers. *Int. J. Mater.* **2020**, *7*. <https://doi.org/10.46300/91018.2020.7.1>.
13. Rühle, S. Tabulated Values of the Shockley-Queisser Limit for Single Junction Solar Cells. *Sol. Energy* **2016**, *130*, 139–147. <https://doi.org/10.1016/j.solener.2016.02.015>.
14. Omarova, Z.; Yerezhep, D.; Aldiyarov, A.; Tokmoldin, N. In Silico Investigation of the Impact of Hole-Transport Layers on the Performance of  $\text{CH}_3\text{NH}_3\text{SnI}_3$  Perovskite Photovoltaic Cells. *Crystals* **2022**, *12*, 699. <https://doi.org/10.3390/cryst12050699>.
15. Du, H.J.; Wang, W.C.; Zhu, J.Z. Device Simulation of Lead-Free  $\text{CH}_3\text{NH}_3\text{SnI}_3$  Perovskite Solar Cells with High Efficiency. *Chinese Phys. B* **2016**, *25*, 108802. <https://doi.org/10.1088/1674-1056/25/10/108802>.
16. Reyes, A.C.P.; Lázaro, R.C.A.; Leyva, K.M.; López, J.A.L.; Méndez, J.F.; Jiménez, A.H.H.; Zurita, A.L.M.; Carrillo, F.S.; Durán, E.O. Study of a Lead-Free Perovskite Solar Cell Using CZTS as HTL to Achieve a 20% PCE by SCAPS-1D Simulation. *Micromachines* **2021**, *12*, 1508. <https://doi.org/10.3390/mi12121508>.
17. Dang, Y.; Zhou, Y.; Liu, X.; Ju, D.; Xia, S.; Xia, H.; Tao, X. Formation of Hybrid Perovskite Tin Iodide Single Crystals by Top-Seeded Solution Growth. *Angew. Chemie-Int. Ed.* **2016**, *55*, 3447–3450. <https://doi.org/10.1002/anie.201511792>.

18. Ahamed, T.; Rahaman, I.; Karmakar, S.; Halim, A.; Kumar, P. Thickness Optimization and the Effect of Different Hole Transport Materials on Methylammonium Tin Iodide ( $\text{CH}_3\text{NH}_3\text{SnI}_3$ )-Based Perovskite Solar Cell. *Emergent Mater.* **2022**, *6*, 175–183. <https://doi.org/10.1007/s42247-022-00405-8>.
19. Zandi, S.; Razaghi, M. Finite Element Simulation of Perovskite Solar Cell: A Study on Efficiency Improvement Based on Structural and Material Modification. *Sol. Energy* **2019**, *179*, 298–306. <https://doi.org/10.1016/j.solener.2018.12.032>.
20. Bouri, N.; Talbi, A.; Khaaissa, Y.; Derbali, S.; Bouich, A.; Nouneh, K. Insight into  $\text{MAPb}_{1-x}\text{Eu}_x\text{I}_3$  Based Perovskite Solar Cell Performance Using SCAPS Simulator. *Optik* **2022**, *271*, 170235. <https://doi.org/10.1016/j.ijleo.2022.170235>.
21. Hasnain, S.M. Examining the Advances, Obstacles, and Achievements of Tin-Based Perovskite Solar Cells: A Review. *Sol. Energy* **2023**, *262*, 111825. <https://doi.org/10.1016/j.solener.2023.111825>.

**Disclaimer/Publisher's Note:** The statements, opinions and data contained in all publications are solely those of the individual author(s) and contributor(s) and not of MDPI and/or the editor(s). MDPI and/or the editor(s) disclaim responsibility for any injury to people or property resulting from any ideas, methods, instructions or products referred to in the content.